Hydrodynamic Analysis of A Rim-driven Thruster Based on RANS Method

Minjian Cai, Canjun Yang*, Shijun Wu, Yushi Zhu, Yu Xie
State Key Laboratory of Fluid Power Transmission and Control, Zhejiang University
Hangzhou 310027, China
*Corresponding author. Tel.: 86-571-87953759; Fax: 86-571-87953759; *Email address*: ycj@zju.edu.cn

***Abstract*—Rim-driven thruster is gaining wide attention in applications such as underwater vehicles and low-speed vessels. Literature on the influence of rotating rim and the rim-fixed blades on performance is scanty. In this paper, a rim-driven propeller was modeled with its hydrodynamic performance numerically simulated by a commercial Reynolds-averaged Navier-Stokes equation solver. The influence of rim on the wake field and friction loss was studied by simulations using rims of different lengths. The results show a long rim will increase friction torque slightly and will induce a circumferential velocity to the local flow, which means at blade tip region the relative tangential velocity of inflow to the blade section reduces and the pitch angle increases. Analysis of the pressure contours indicates the rim-driven propeller is easier to cause cavitation problem if directly modified from Ka-series. In addition, a following blade thickness study shows the thin blade has an efficiency advantage over the thick one.**

Keywords—computational fluid dynamics; hydrodynamics; underwater propulsion; rim-driven; rim effect

I. Introduction

A rim-driven propeller (RDP), or tip-driven propeller (TDP) in some other references, is a kind of propeller with its blades driven by a rotor whose inner surface permanently attached to the tips of the blades other than by a shaft connecting to the hub. Although the concept has been proposed for a long time [1], it is not until recent years that it becomes actually practical due to the development of advanced material, electric machine design and manufacturing technology.

RDP eliminates its driving shaft and corresponding accessories like seals, bearings and gear boxes by locating a electric motor and support structures in the duct, thus makes itself a compact and low maintenance cost component. Since there is no block in the inflow, it is less possible to be entangled with marine fouling and it is easier for a RDP to achieve symmetric port and starboard thruster performance. Besides, the elimination of tip clearance increases the tip circulation, which can help to produce higher thrust than ordinary one [2]. These characteristics make it very attractive to applications such as underwater vehicles and bow thruster.

Now we can see that the RDPs feature a number of hydrodynamic and structural advantages over conventional types of propellers. However, for such a new propeller, some of the issues of design and performance analysis need to be studied. Sharkh and Turnock gave an overview of the general design philosophy and practical issues, and meanwhile, they designed a demonstrator RDP with the performance results presented [3]. Detailed structure and mechanical considerations were described and the influence of duct section shape was investigated, but the hydrodynamic aspects were little involved. The importance of matching of motor and propeller characteristics was stressed in achieving an efficient design. Yakovlev and Sokolov carried out a comparison study of two RDP blading systems, namely rim-fixed (hubless) type and hub-fixed type, with an optimized blade pitch distribution over radius [4]. The blade strength analysis showed there is reduction of stress levels and bending moment in the case of rim-fixed blades. Open water performance and cavitation characteristics were also investigated for both of the cases. Hsieh et al. designed a rim-driven thruster for remotely operated vehicles [5]. Their design process considered the integration of propeller design and motor design. A prototype was manufactured and tested, although the output does not achieve its intended values due to high friction loss.

On the other hand, in order to assess the performance of a RDP, researches on performance analysis and prediction were carried out. Cao et al. employed a commercial Reynolds-averaged Navier-Stokes (RANS) equation solver to predict the steady wake field and loading distributions for a RDP [6]. Four different pitch ratio distributions were analyzed and compared. Though the rim, as well as the air gap, was not modeled in the geometry, the hydrodynamic influences of the rim surface were taken into account by empirical corrections. The numerical results showed that due to the structural features, there is increased circulation in tip region. Kinnas et al. analyzed the unsteady flow of a rim-driven thruster by an approach that combined a vortex-lattice method with a RANS solver [7]. The method they used can predict the extent of cavitation well. Amminikutty et al. presented the performance characteristics of a RDP which showed improved thrust delivery and torque absorption can be achieved, though there is no significant improvement of efficiency [8].

Up to now, we can see that some prototypes have been successfully designed and manufactured and some of the main problems like structure design, loading distribution analysis, and performance and cavitation prediction were addressed. In this paper, a RDP model with full rim surfaces and air gap was redesigned based on Kaplan blade and Kort nozzle section, and

978-0-933957-43-5 ©2015 MTS

the commercial RANS solver (FLUENT) was used to calculate the flow field. Influences of rims with different lengths and blades with different thicknesses were studied. Open water performance at varied advance ratios was obtained.

II. Numerical Modeling and Method

A. Model

The rim-driven propeller used in this study was modified from a Kaplan duct propeller which has four blades and the No. 19A nozzle. The propeller is 240mm in diameter (D) with its blades area ratio equals 0.5, and the chord to diameter ratio of the nozzle is 0.5. Details of the Kaplan duct propeller geometry can be found in 【】. The pitch ratio is 1.2 so from the open water test results of Ka 4-55 screws series with nozzle No.19A we can speculate that this RDP may achieve its maximum efficiency at advance number near 0.7. A rectangular opening in the inner surface of the duct is made to fit the rim and gaps in radial and axial direction are all set to 2mm. The differences between the RDP and conventional duct propeller are the additional rim and resulting gap, eliminated hub and blade thickness distribution, as shown in Fig.1.

In an integrated design of RDP, the rim plays an important role in torque and thrust transmission. The size of it may be specifically required due to motor design and mechanical concern, and compromise may need to be considered during the overall design. So we set the length of rim to three different values to study the resulting friction loss and wake field. All the rims are symmetric about the blade reference line. The shortest rim was made just long enough to fit the blade tip while length of the other two increases successively, as shown in Fig.2. In each model, the duct is modified correspondingly to keep the gaps consistent. On the other hand, the blade loads of hydrodynamic sources arise mainly from the blades' outer regions. So it is possible to reduce blades' thickness near the blade joints as in the rim-fixed structure the bending moments could be smaller. Primary research on the blade load has verified the peak stresses in the case of traditional hub-type design can be 1.5 times higher than in the case of rim-fixed blades [4]. In our study, two thickness distributions are applied to investigate its effect on performance. As illustrated in Fig.2, t1 denotes the thickness distribution simply inverted from the hub-driven type, while t2 denotes the model for comparative study.

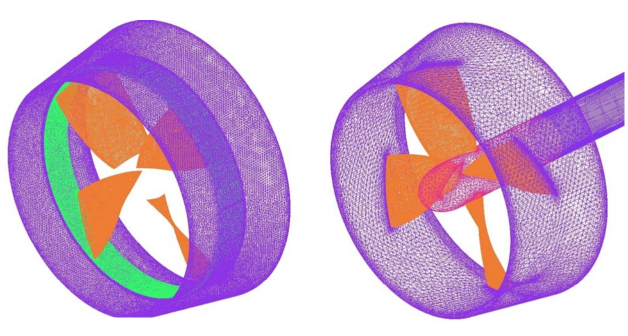

Fig. 1. Left: Rim-driven propeller to be investigated; Right: Ka 4-55 propeller in No.19A nozzle.

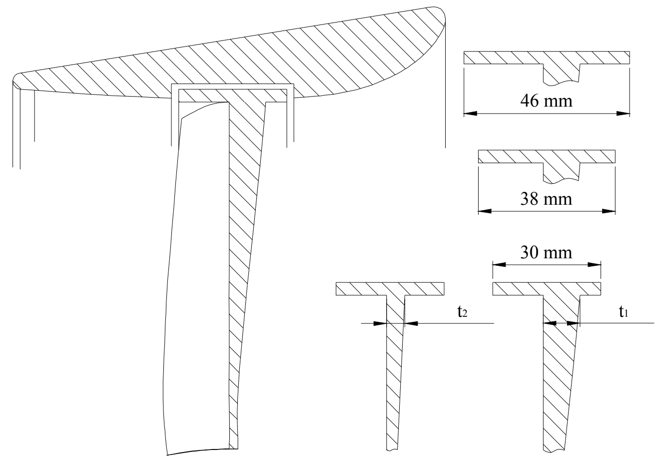

Fig. 2. Corss-section draft of a rim-driven propeller and rims with three length values.

B. Numerical method

In our study, three dimensional RANS equations are applied to calculate the steady flow field around the propeller. The k− ω SST turbulence model is used to solve RANS equations. Pressure and velocity coupling is achieved by SIMPLEC algorithm. Rotating reference frame is used and no-slip condition is applied to the surfaces of blades, rim and duct. The whole computational domain is a cylinder of 5D in diameter and 10D in axial length, with the propeller coaxially locating at 3D near the inlet, as illustrated in Fig.3. The solver (FLUENT) adopts finite volume method to discretely solve the governing equations. To accelerate convergence and ease the burden of computer memory, we divided the computational domain into two different gird type regions. The exterior domain uses structured grid while the interior domain uses unstructured grid to capture the subtle geometric features.

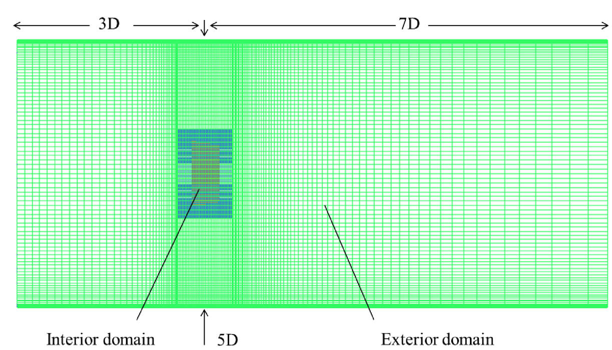

Fig. 3. Illustration of the computational domain.

The detailed flow field information is closely related to grid resolution and the accuracy of viscous drag for a turbulence model is sensitive to the near-wall mesh resolution. It is therefore important to ensure sufficient grid refinement in interested regions. Small edge spacing was applied to blade leading edge, trailing edge and root regions. Gaps and surfaces of tip regions, blades and rim were further refined, because of their influence on grid quality. Suitable prism cell layers are

Identify applicable sponsor/s here. If no sponsors, delete this text box (*sponsors*).

recommended to create near the wall to obtain small y+, however, we directly refined the interested grid regions in this case for that the whole mesh is easier to obtain high quality and meanwhile we can get acceptable y+ values. After a grid dependency study, suitable mesh size was selected and the total number of cells is about 3 million. The final mesh quality is about 0.35.

To validate the numerical calculation, the aforementioned standard Ka 4-55 duct propeller was modeled and calculated. As a result, the simulated open water characteristic showed only little difference exists between the numerical analysis and experimental tests. The average efficiency difference is about 2.5% and the main contribution comes from underestimation of absorbed torque.

III. Results and Discussion

A. Comparsion with Ka-series Propeller

A comparison between RDP and the traditional Ka-series propeller (with a tip gap of 2.5mm) was drawn. CFD simulations are conducted under different load conditions with advance ratio (*J*) ranges from 0.07 to 1.0. The value 0.07 is selected because advance ratio close to zero is hard to converge for the solver. An arbitrary rotational speed of 120 rad/s was selected and the corresponding freestream velocities were respectively chosen on the definition of *J*.

Fig. 4 shows the blade pressure distribution at advance ratio $J = 0.7$. It can be seen that pressure contours of blade regions near the root are about the same while the obvious difference exists in the middle to tip radii regions. The eliminated gap between blade tip and duct helps increase the blade tip and duct circulation and thus expands the pressure difference between suction surface and pressure surface. However, it is odd that on the pressure surface of RDP, pressure near the leading edge is unusual low, and on the contrary, the pressure near leading edge on the suction surface is high. This will definitely affect the performance since the cavity bubbles in the pressure face are easy to cause thrust breakdown, let alone the noise and erosion problems. We ascribe this local pressure phenomenon to two possible reasons: the first is that blade sections of outer radii in the Ka-series are flat on pressure surface and the directly inverted thickness distribution of the Ka-series propeller makes the blade tip much thicker than ordinary blade and then lead to an unsuitable geometry; the second is that the rim structure affects local flow since the boundary layer of the rim will introduce a superimposed velocity on the tangential inflow velocity. This could be seen from a velocity diagram that the relative tangential velocity of inflow to propeller decreases when the local fluid has a velocity with the same direction. As a result, the angle of attack at the local blade sections may turn negative. Fig.5 presents predicted open water characteristics for RDP and the Ka-series propeller in No. 19A nozzle where the cavitation effect has not been taken into consideration. The results show that the RDP can produce higher thrust under different load conditions, though at the cost of absorbing higher torque from the prime engine. As a result, the efficiency is lower than a conventional hub-driven type. This is consistent with the experimental result from existing researches.

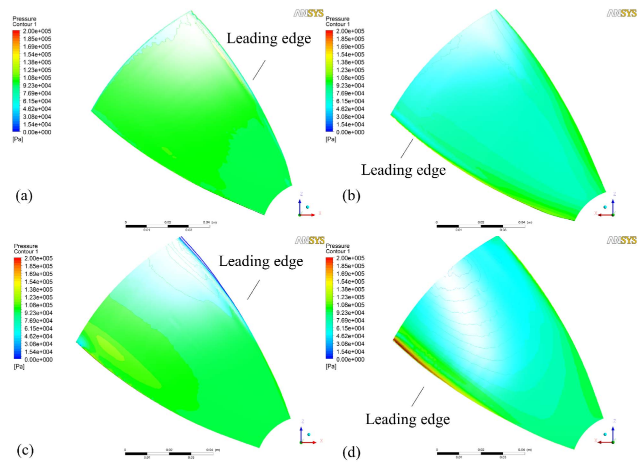

Fig. 4. Pressure contours at advance ratio $J = 0.7$: (a) pressure surface of Ka-series propeller; (b) sucction surface of Ka-series propeller; (c) pressure surface of RDP; (d) suction surface of RDP;

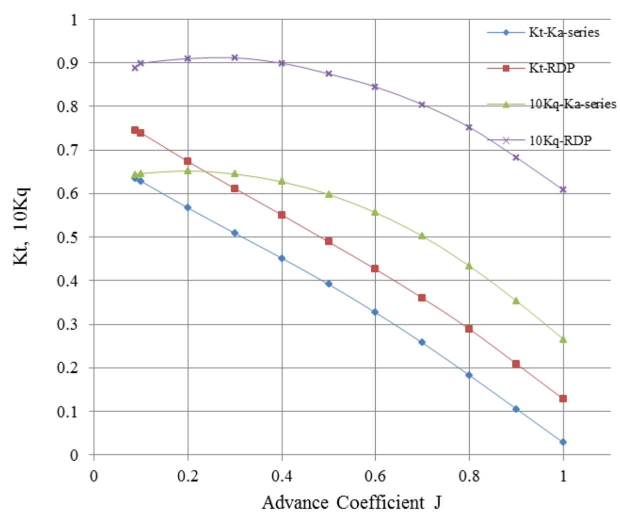

Fig. 5. Pridicted open water characteristics.

The absorbed torque of a RDP can be divided into two parts: one comes from the rim surfaces and the other comes from the blades surfaces. Reports of the results indicate that the torque produced from rim rises slowly as the advance ratio increases, and the proportion of that also increases. This is because in the low inflow velocity condition, notable form resistance of blades will produce while the friction from the inner surface of rim keeps low due to the relative low velocity. The proportion of rim friction torque is 4.7% at $J = 0.1$ and is 6.8% at $J = 0.8$, which is not very high in this case. Nevertheless, it should be noted that the rim friction loss has a close relationship with the duct gap length and rotation speed. So a compromise will be made when design the rim motor.

B. Influence of The Rim Length

Beside the friction, the rim also has a potential influence on the wake field especially when the rim is long. When the rim rotates, the boundary layer of it flows downstream. So a circumferential velocity component is introduced into the local flow near the blade tip. To investigate the influence on the wake, three rims with different lengths were used in our study. The wake fields are illustrated below.

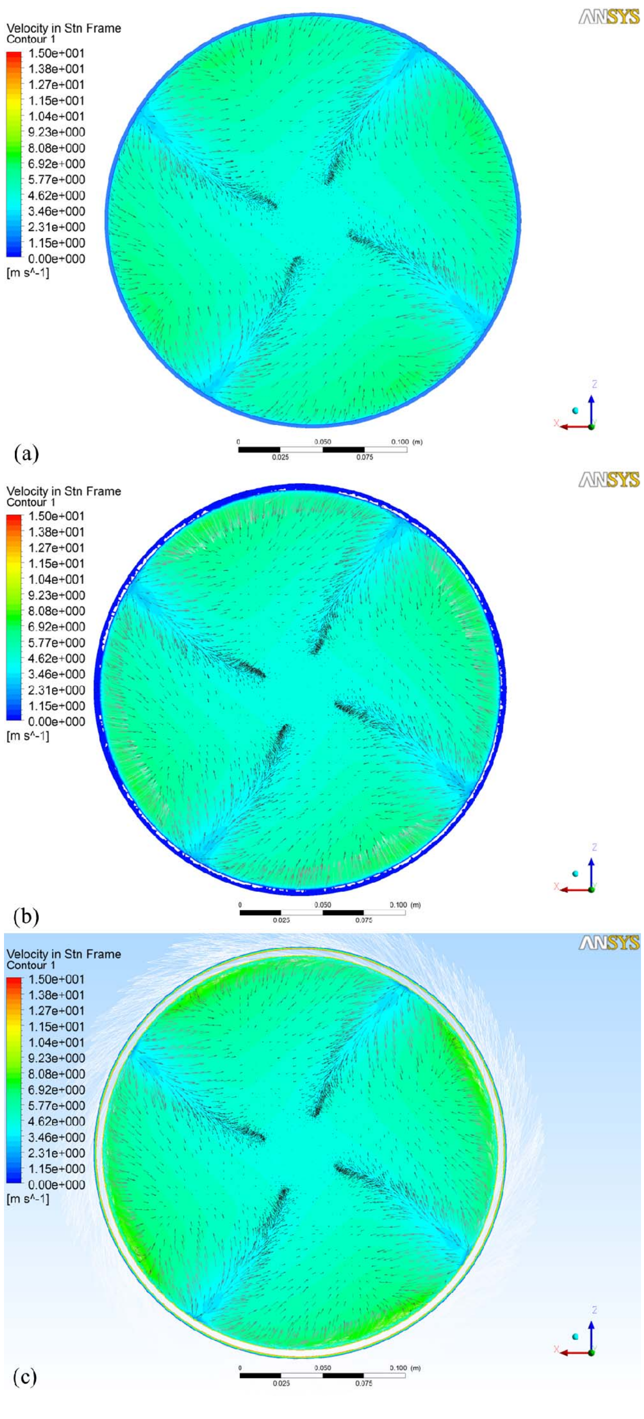

Fig. 6. Wake flow of evaluating suface at y = 0.18R upstream: (a) rim length is 30 mm; (b) rim length is 38 mm; (c) rim length is 46 mm.

The results show when the length increases, circumferential velocities of the fluid in the near-rim region increase as we expected. This is obvious in the near wall though the overall flow field has not been affected. So some local modification may be needed in the detailed design of a rim-driven blade especially when the rim is not short. It should be noted that the blue rims in (a) and (b) denotes the region of axial gap between rim and duct. In addition, the friction brought by the rim also increases with length, from 5.7% (30mm) of the total torque to 7.8% (46mm).

C. Blade Thickness Study

Thickness influence on the open water performance was studied by adopting two kinds of thickness distribution as tabulated in Table I, where one (RDP1) is simply inverted from the Ka-series propeller while the other (RDP2) is further modified to reduce the blade thickness.

TABLE I. THICKNESS DISTRIBUTION

	Maximum blade thickness in percentages of the diameter		
r/R	**Ka-series Propeller**	**Rim-driven propeller 1**	**Rim-driven propeller 2**
0.2	4.00	0.50	0.50
0.3	3.52	0.61	0.56
0.4	3.00	0.92	0.71
0.5	2.45	1.38	0.96
0.6	1.90	1.90	1.14
0.7	1.38	2.45	1.36
0.8	0.92	3.00	1.57
0.9	0.61	3.52	1.79
1.0	0.50	4.00	2.00

Open water performance results from CFD simulations are shown in Fig.7. A little improvement on efficiency can be obtained by reducing the blade thickness, which enlightens us the using of high-strength material for high load condition. By checking the pressure contours we found zero pressure at the leading edge (like that of Fig.4) still exists, however, the area of low pressure in pressure surface contracts which means the cavitation situation can be improved.

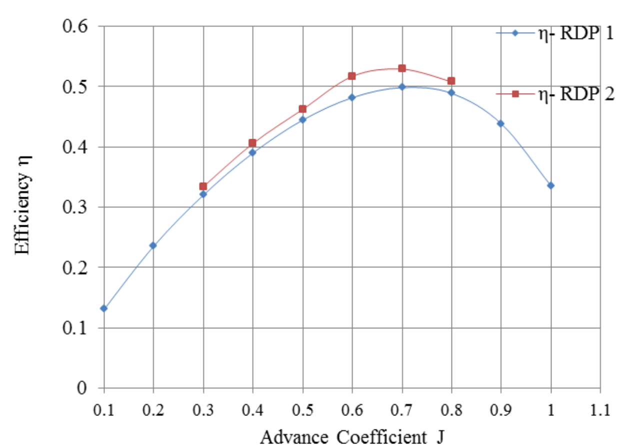

Fig. 7. Open water performance results of two sets of thickness distribution.

IV. CONCLUTION AND FURTURE WORK

In this paper, a rim-driven propeller was modeled and its performance was numerically simulated. The numerical modeling method is discussed and verified by a Ka-series propeller. Comparison between a rim-driven propeller and a hub-driven propeller was drawn and the results show the rim-driven propeller can produce more thrust with little compromising on efficiency. The situation can be improved by using thinner blade since a following blade thickness study indicates the thin blade has an advantage over the thick one. Results show that cavitation problem can be serious in a RDP if we do not carefully deal with. Besides, rim effects on both friction and wake field were studied. The results indicate a long rim will increase friction torque slightly and will introduce a circumferential velocity to the local flow. This means at the blade tip the relative tangential velocity to the blade section reduces and the angle of attack decreases.

Due to time limits, the analysis of the blade thickness influence is not comprehensive for some simulations are still running. In the future, we plan to design a prototype that will take these effects into consideration by the advanced lifting surface method.

ACKNOWLEDGMENT

The authors are grateful to the State Key Lab of Fluid Power Transmission and Control of Zhejiang University for providing workstation. In addition, the authors gratefully acknowledge the financial support of the Science Fund for Creative Research Groups of National Natural Science Foundation of China (No.51221004) and the Program for Zhejiang Leading Team of S&T Innovation (Granted No.2010R50036).

REFERENCES

[1] Wardell G S. Retractable bow thruster: U.S. Patent 4,294,186[P]. 1981-10-13.

[2] Baltazar J, J. A. C. Falcao de Campos, Bosschers J, “Open-Water Thrust and Torque Predictions of a Ducted Propeller System with a Panel Method,” International Journal of Rotating Machinery, vol. 2012, Article ID 474785, 11 pages, 2012.

[3] Sharkh S M A, Turnock S R, Hughes A W, “Design and performance of an electric tip-driven thruster,” Proceedings of the Institution of Mechanical Engineers, Part M: Journal of Engineering for the Maritime Environment, 2003, 217(3): 133-147.

[4] Yakovlev A Y, Sokolov M A, Marinich N V, “Numerical design and experimental verification of a rim-driven thruster,” Proceedings of Second International Symposium on Marine Propulsors. Hamburg, Germany. 2011.

[5] Hsieh M F, Chen J H, Yeh Y H, et al, “Integrated design and realization of a hubless rim-driven thruster,” Industrial Electronics Society, 2007. IECON 2007. 33rd Annual Conference of the IEEE. IEEE, 2007: 3033-3038.

[6] Cao Q, Hong F, Tand D, et al, “Prediction of loading distribution and hydrodynamic measurements for propeller blades in a rim driven thruster,” Journal of Hydrodynamics, Ser. B, 2012, 24(1): 50-57.

[7] Kinnas S A, Chang S H, He L, et al, “Performance prediction of a cavitating RIM driven tunnel thruster,” Proceedings of the First International Symposium on Marine Propulsors, SMP. 2009, 9: 435-442.

[8] Amminikutty V, Subramanian V A, Dhinesh G, “Dynamic Characteristics of Marine Hubless Screw Propellers,” 2006.

[9] Carlton J. Marine propellers and propulsion. Butterworth-Heinemann, 2012.